COMPUTATION OF ELECTRON DIODE CHARACTERISTICS BY MONTE CARLO METHOD INCLUDING EFFECT OF COLLISIONS

by Charles M. Goldstein

Lewis Research Center
Cleveland, Ohio

TECHNICAL PREPRINT prepared for

Thermionic Conversion Specialist Conference sponsored by the
Institute of Electrical and Electronics Engineers
Cleveland, Ohio, October 26-28, 1964

NATIONAL AERONAUTICS AND SPACE ADMINISTRATION

TM X-52070

COMPUTATION OF ELECTRON DIODE CHARACTERISTICS BY MONTE CARLO METHOD INCLUDING EFFECT OF COLLISIONS

by Charles M. Goldstein

Lewis Research Center
Cleveland, Ohio

Abstract

A consistent-field Monte Carlo Method is presented for the calculation of electron (and/or ion) diode characteristics including the effect of collisions. The method is applied to two cases of electron flow through a perfect Lorentzian gas - monoenergetic emission, and thermionic emission. Hard sphere elastic collisions are assumed between electrons and neutral gas molecules. Electron density distributions, potential distributions, and current-voltage characteristics are presented for both cases. The effect of increased mean-free-path on the aforementioned characteristics is discussed.

Introduction

This paper presents a new method for determining the effect of collisions on diode characteristics and discusses the application of this method to determine the effect of elastic, hard sphere electron-neutral collisions for both monoenergetic and thermionic emission. The method is, essentially, a consistent-field computor simulation (Monte Carlo method) of the physical model. The Monte Carlo Method has, in recent years, been employed with considerable success to a wide variety of problems[1], most notably in the area of nuclear shielding problems (viz., neutron transport). These latter problems are linear in the sense that the transport of neutrons is independent of the particle density. More recently, the method has been extended to certain nonlinear problems in radiation transport[2]. Other computor-simulated solutions of nonlinear problems in molecular dynamics[3] and plasma physics[4] approximate the physical model by a large number of particles or current sheets, which are then followed deterministically through all mutual interactions by the computer. For many problems such methods are not practical because of computor storage and speed limitations.

Just as the nonlinearity in the radiation transport problem is characterized by a single parameter, the temperature[2], so the nonlinearity in charged-particle transport problems is characterized by a single parameter, the potential. Unlike the photons in the former problem, however, the charged particles experience a body force proportional to the first derivative of the potential.

The electron transport problem is solved herein in the following manner. An initial potential distribution is assumed. A large number of independent electrons are then followed through their trajectories under the influences of both the potential field and collisions. The contribution to the charge density made by each electron is tallied at preassigned data points in the interelectrode region. In addition, the number of electrons reaching the collector is tallied. At the end of one iteration, a density distribution is obtained by fitting a curve to the densities at the data points. A new potential distribution is obtained by solving Poisson's equation for the given density distribution. The procedure is then repeated for a given number of successive iterations. Convergence is obtained in the initial iterations; succeeding iterations are then employed as independent trials. The final step is to obtain the mean and standard deviation of the collector currents resulting from the independent trials.

Langmuir[5] published the first correct solution to the effect of space-charge and initial velocities on the potential distribution and thermionic current between parallel plane electrodes. He also studied the problem of diffusion of electrons back to the emitter for the case of very small mean-free-paths[6]. The Monte Carlo solutions presented herein are an extension of these results to the case for which the mean-free-path is not necessarily small with respect to the interelectrode separation.

Monte Carlo Calculations

The following equations and dimensionless variables will be employed in the subsequent discussion:

$$\varphi''(y) = Cn(y) \tag{1}$$

$$y \equiv x/L \tag{2}$$

$$n \equiv \hat{n}/n_o \tag{3}$$

$$l \equiv S/L \tag{4}$$

$$\alpha \equiv L/\lambda \tag{5}$$

$$\varphi \equiv \frac{2eV}{mv_o^2} \tag{6a}$$

$$\varphi \equiv \frac{eV}{kT} \tag{6b}$$

$$C = 8\pi eL^2 J_o/mv_o^3 \tag{7a}$$

$$C = 16(\pi/2hT)^{3/2}\, m^{1/2}\, eJ_o L^3 \tag{7b}$$

$$u \equiv v_x/v_o \tag{8a}$$

$$u \equiv v_x/v_{th} \tag{8b}$$

$$V \equiv v_T/v_o \tag{9a}$$

$$V \equiv v_T/v_{th} \tag{9b}$$

where equation (1) is Poisson's equation in dimensionless variables, x is the distance along the normal to the emitter, L is the interelectrode spacing, $\hat{n}$ is the electron density, n_o is the emitted electron density at $x = 0$, $mv_o^2/2e$ is the initial energy of monoenergetic emission, kT/e is the thermionic emitter temperature, J_0 is the emitted current density, s is the distance along a trajectory, λ is the mean-free-path, v_x is the velocity component in the x-direction, v_T is the velocity component transverse to the x-direction, and $v_{th} = \sqrt{2kT/m}$. Equations (a) and (b) refer to monoenergetic and thermionic emission, respectively.

Initial Conditions

For monoenergetic emission, each test particle is emitted with the same energy and vector velocity (normal to the plane of the emitter). For thermionic emission, the initial velocities must be chosen from the distribution of flux in velocity space

$$\sqrt{\pi}\, uf(u,V)du\, dV \tag{10}$$

where

$$f(u,V)du\, dV = (4/\pi)Ve^{-(u^2 + V^2)}du\, dV \tag{11}$$

is the half-Maxwellian distribution of the emitted electrons. (Note that, although one speaks of test "electrons," the statistics are obtained for units of flux - not units of charge density.) In applying the Monte Carlo technique, two random numbers, R_1 and R_2, are chosen from a uniform distribution, and the following equations are used for u and V[7]:

$$u^2 = -\ln(R_1)$$

$$v^2 = -\ln(R_2) \tag{12}$$

Distance to Collision

The assumptions of hard sphere collisions and a perfect Lorentzian gas of target particles imply a constant mean-free-path λ and isotropic scattering in the laboratory system[8]. Hence, the probability of an electron suffering a collision in distance l is

$$1 - e^{-\alpha l} \tag{13}$$

The distance to collision along the trajectory of a given test particle is obtained by choosing a random number R and solving[9]

$$l_c = -(1/\alpha) \ln (R) \tag{14}$$

For monoenergetic emission, no collision will occur if the initial distance to collision l_c is greater than one. This is not true, in general, for thermionic emission, since l_c is then the non-dimensionalized path length along a curvilinear trajectory.

The actual computation of distance along a trajectory was accomplished by a combination of Gaussian quadratures with weights one[10] and $1/\sqrt{x}$,[11] and Simpson's Rule[12]. The $1/\sqrt{x}$-weighted Gaussian quadrature was employed for numerical integrations past a turning point (where the u-component of velocity becomes zero), since such integrations involved a singular integrand of strength $1/\sqrt{u}$.

Scattering Angle

After a collision occurs, the cosine of the random scattering angle is obtained from

$$\cos \theta = 1 - 2R \tag{15}$$

where R is, once again, a random number chosen from a uniform distribution.

Density

The contribution to the density at each data point y_i of a unit of flux of velocity $u(y_i)$ is

$$n(y_i) = 1/\sqrt{\pi}\, u(y_i)$$

$$u(y_i) = \sqrt{u_o^2 + \varphi(y_i) - \varphi(y_o)} \tag{16}$$

where y_o is the dimensionless position of the last "event" (emission or collision) and u_o is the dimensionless velocity component at the start of the new trajectory.

The sample density at data point y_i for a total of N_o histories is then

$$n(y_i) = \frac{1}{\sqrt{\pi}\, N_o} \sum_k \frac{1}{u_k(y_i)} \tag{17}$$

where the sum over k may be greater than, equal to, or less than N_o because of collisions and turning points in the trajectories caused by the potential field.

Current to Collector

The ratio of current density to the collector J to the emitted current density J_o for

each iteration is computed from the relation

$$J/J_o = N_c/N_o \tag{18}$$

where N_c is the number of test electrons reaching the collector.

Results

Thermionic Emission

The effect of mean-free-path on the current-voltage characteristic is shown in Fig. 1. The solid line, $L/\lambda = 0$, represents the collisionless solution of Langmuir[5]. The Monte Carlo calculations indicated along this curve were undertaken as a check on the computor program. These particular results were obtained with 5000 histories per iteration, and ten iterations. The execution time for each point on the curve varied between 2.5 and 4.0 minutes.

The two solid data points on the curves for $L/\lambda = 1$ and 5 represent the conditions where the slope of the potential is zero at the emitter. The X's on the curve $L/\lambda = 1$ indicate the results of an independent solution of Boltzmann's transport equation for this problem (presented in the paper by P. M. Sockol).

The effect of potential on the electron density distribution for $L/\lambda = 5$ is shown in Fig. 2. From the emitter out to about one mean-free-path, the density of the higher energy electrons is less than that of the lower energy electrons as would be expected under conditions of no collisions. Beyond one mean-free-path, however, the situation is reversed. This is caused by the increase in the number of collisions suffered by the higher energy electrons; increased collisions result in a slower drift velocity even though the accererating potential is higher. High-energy electrons undergo more collisions than low-energy electrons because they will, in general, travel longer distances parallel to the electrode surfaces. (This also implies a greater loss rate out the sides in a finite-dimension system.)

The effect of mean-free-path on the density and potential distributions for constant collector potential are shown in Figs. 3 and 4, respectively. As expected, the effect of collisions is to increase the charge density and, therefore, decrease the potential in the interelectrode space.

Monoenergetic Emission

The corresponding diode characteristics for monoenergetic emission are shown in Figs. 5 to 8. The author has, at present, no hypothesis regarding the inflections observed in the current-voltage characteristics (Fig. 5) for $L/\lambda = 0.5$ and 1.0. The points calculated are reproducible, and each point, as plotted, spans at least plus or minus two standard deviations about the mean J/J_o.

The other most noteworthy feature of the monoenergetic emission characteristics is the buildup of charge density in the interelectrode region as the potential is decreased (Fig. 6). This increase in charge density is considerably enhanced by the appearance of a potential minimum (cf. upper curve in Fig. 6). The potential minimum causes more turning points to occur in the trajectories of the scattered electrons. Since the u-component of velocity becomes zero at a turning point, the contribution to the charge density of electrons undergoing reflections in the potential field is exceptionally high.

Discussion

Some typical statistics are presented in Table I. The standard deviation about the mean J/J_o taken over the given number of iterations is represented by σ_J. Most striking is the effect of the consistent-field constraint (Poisson's equation) on the number of histories needed for reasonable statistics. In the last two rows of the table, it can be seen that the effect of sample size (number of histories) on the standard deviation is significantly less than would be expected in a linear problem.

The present computor program is optimized for small L/λ. In the third row from the bottom in Table I, it is apparent that any additional increase in L/λ would be very costly in computor time with the present program. In addition to optimizing this program for large values of L/λ, there exist other techniques, such as the introduction of "weight parameters,"[14] which show great promise of reducing the necessary execution times. The computations presented in this report were done on an IBM 7094 Model II computor, and the programs were written in FORTRAN IV.

Although the results presented in this paper employed a simple hard sphere collision model, the great advantage in this method lies in its inherent ability to provide similar solutions for any given collision-model, theoretical or experimental. This includes inelastic, charge exchange, and ionizing collisions. This method is limited, however, to those cases where avalanche ionization does not occur.

References

1. Kraft, R., and Wensrich, C. J.: "Monte Carlo Methods, A Bibliography Covering the Period 1949 to 1963" UCRL-7823 (1964)

2. Fleck, J. A., Jr.: "The Calculation of Nonlinear Radiation Transport by a Monte Carlo Method" in "Methods in Computational Physics", Vol. I, Academic Press (1963), pp. 43-65.

3. Alder, B. J., and Wainwright, T.: "Molecular Dynamics by Electronic Computors" in "Proc. Intern. Symposium on Transport Processes in Statistical Mechanics", Wiley (Interscience) (1957) pp. 97-131.

4. Burger, P.: "The Opposite-Stream Plasma Diode", Stanford Electronics Lab. Rept. No. SEL-64-012 (1964), pp. 41 ff.

5. Langmuir, I.: Phys. Rev., XXI, 419 (1923); also in "The Collected Works of Irving Langmuir" Pergamon Press (1961), pp. 95-110.

6. Langmuir, I., and Jones, H. A.: Phys. Rev., XXXI, 357 (1928); Ibid., Vol. 5, pp. 60-110.

7. Haviland, J. K.: MIT Fluid Dynamics Laboratory Rept. No. 61-5 (1961); (AD 259672), pp. 41.

8. Kennard, E. H.: "Kinetic Theory of Gases", McGraw-Hill (1938), pp. 101 ff.

9. Cashwell, E. D., and Everett, C. J.: Los Alamos Scientific Lab. Rept. No. LA-2120 (1957), pp. 49 ff.

10. Abramowitz, M., and Stegun, I. A.: "Handbook of Mathematical Functions" NBS AMS 55 (1964) pp. 916.

11. Krylov, V. I.: "Approximate Calculation of Integrals", Macmillan (1962), pp. 121.

12. Scarborough, J. B.: "Numerical Mathematical Analysis", John Hopkins Press (1962), 5th Ed., pp. 137.

TABLE I. EFFECT OF VARIOUS PARAMETERS ON STANDARD DEVIATION AND EXECUTION TIME.

	L/λ	$\varphi(1)$	J/J_0	σ_J	SAMPLE SIZE	NUMBER OF ITERATIONS	COLLISIONS (FOR ONE ITERATION)	EXECUTION TIME, MIN
B	0.1	0.75	0.961	0.001	5,000	10	483	2.42
		2.0	.972	.0012	5,000	10	503	2.46
		2.0	.971	.0019	2,000	5	213	.51
		4.0	.986	.0005	10,000	10	1,079	5.28
B	.5	4.0	.918	.0015	2,000	10	1,257	2.48
B	1.0	4.0	.839	.0015	1,000	10	1,483	2.09
T	5.0	32.0	.672	.003	1,000	18	16,367	37.65
T	.1	10.2	.942	.0016	1,000	10	147	1.49
		10.2	.942	.0008	10,000	10	1,198	14.18

CS-33966

B ≡ ELECTRON BEAM
T ≡ THERMIONIC EMISSION

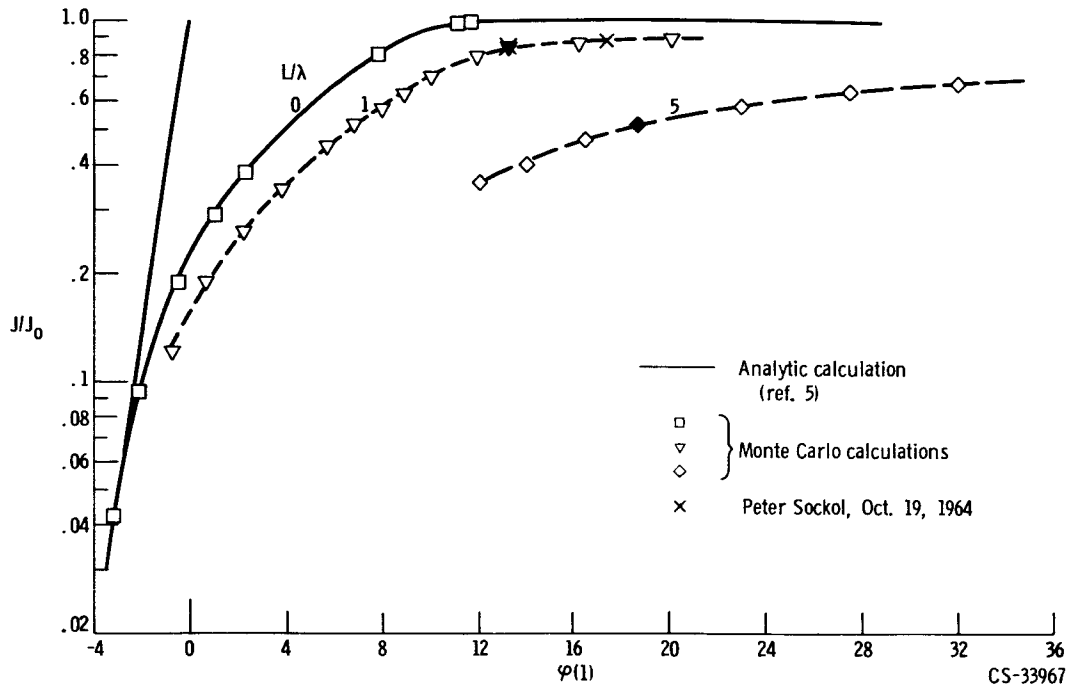

Fig. 1. Effect of mean-free-path on current-voltage characteristics for thermionic emission. C = 50.

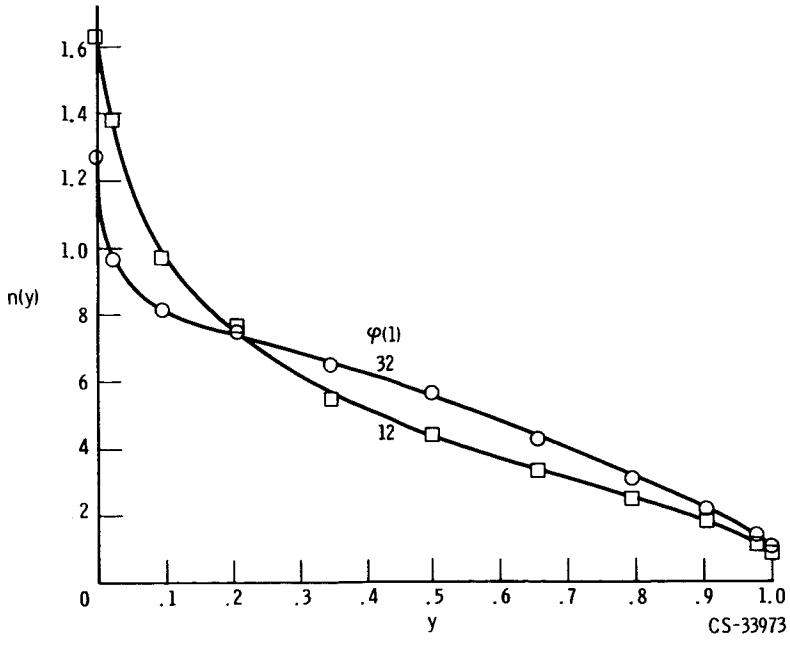

Fig. 2. Effect of anode potential φ(1) on electron density distribution for thermionic emission. C = 50; L/λ = 5.

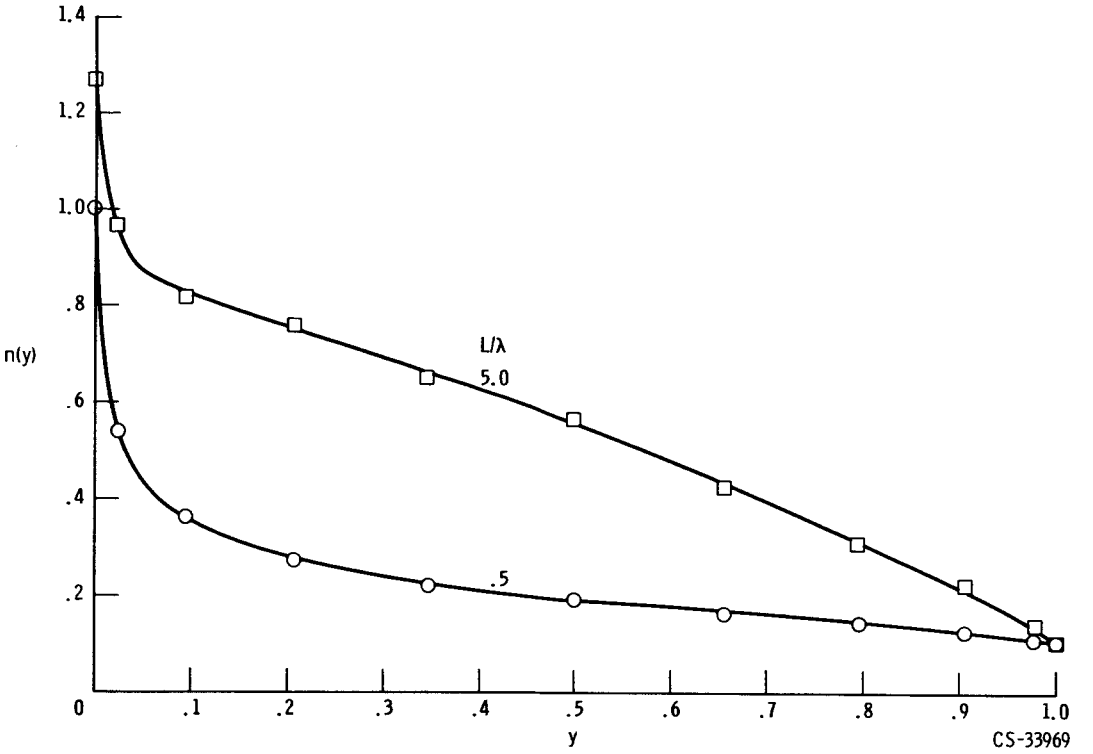

Fig. 3. Effect of mean-free-path on electron density distribution for thermionic emission. C = 50; φ(1) = 32.

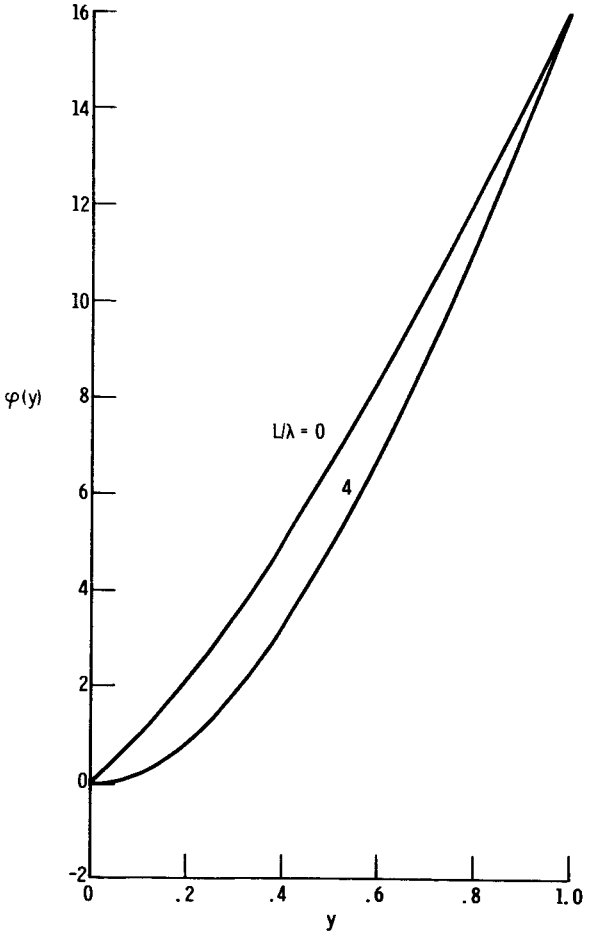

Figure 4. - Effect of mean-free-path on potential distribution for thermionic emission. C = 50.

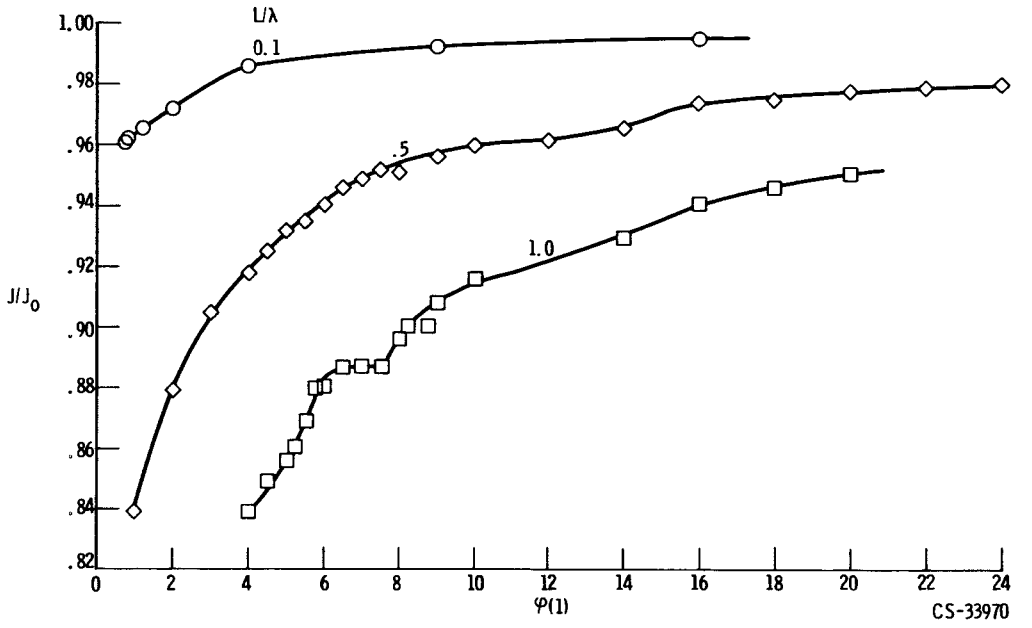

Fig. 5. Effect of mean-free-path on current-voltage characteristics for electron beam. $C = 10/\sqrt{\pi}$.

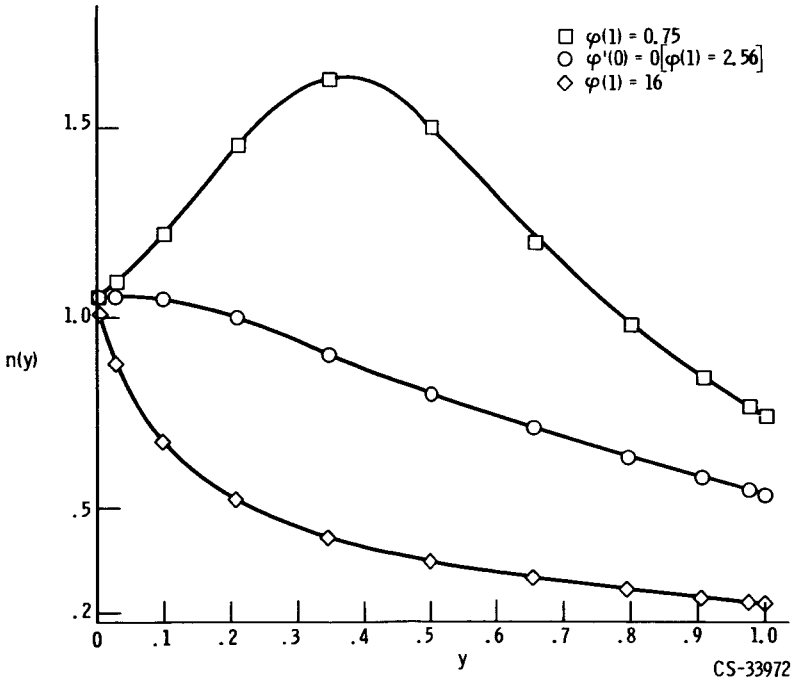

Fig. 6. Effect of anode potential on electron density distribution for electron beam. $C = 10/\sqrt{\pi}$; $L/\lambda = 0.1$.

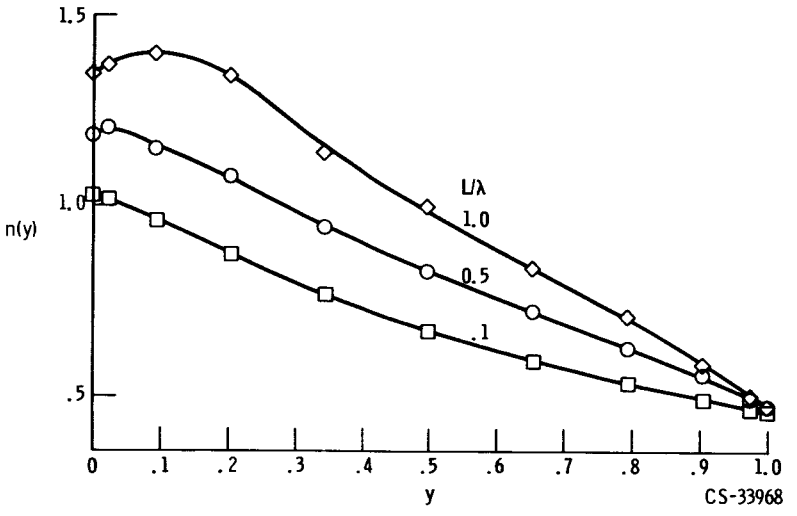

Fig. 7. Effect of mean-free-path on electron density distribution for electron beam. $C = 10/\sqrt{\pi}$; $\varphi(1) = 4$.

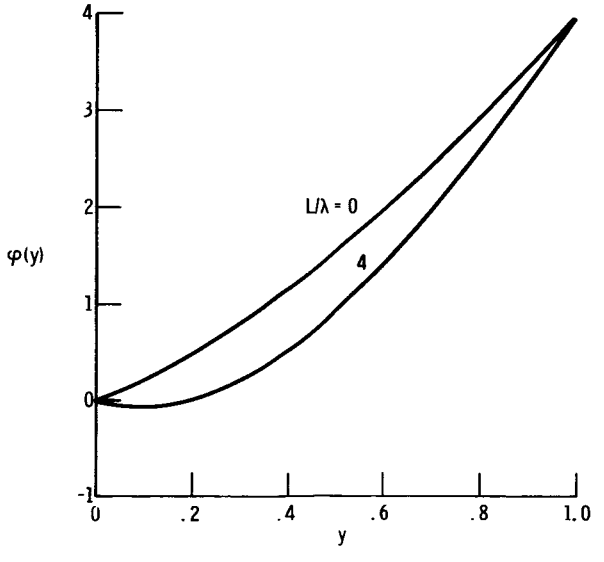

Figure 8. - Effect of mean-free-path on potential distribution for monoenergetic emission. $C = 10/\sqrt{\pi}$.